

Large Scale Urban Simulations with FCT

Gopal Patnaik, Jay P. Boris, Fernando F. Grinstein, John P. Iselin,
and Denise Hertwig

Abstract Airborne contaminant transport in cities presents challenging new requirements for CFD. The unsteady flow physics is complicated by very complex geometry, multi-phase particle and droplet effects, radiation, latent and sensible heating effects, and buoyancy effects. Turbulence is one of the most important of these phenomena and yet the overall problem is sufficiently difficult that the turbulence must be included efficiently with an absolute minimum of extra memory and computing time. This paper describes the Monotone Integrated Large Eddy Simulation (MILES) methodology used in NRL's FAST3D-CT simulation model for urban contaminant transport (CT) (see Boris in *Comput. Sci. Eng.* 4:22–32, 2002 and references therein). We also describe important extensions of the underlying Flux-Corrected Transport (FCT) convection algorithms to further reduce numerical dissipation in narrow channels (streets).

1 Background

Urban airflow accompanied by contaminant transport presents new, extremely challenging modeling requirements. Configurations with very complex geometries and

G. Patnaik (✉) · J.P. Boris
LCP&FD, Naval Research Laboratory, Washington, DC 20375, USA
e-mail: patnaik@lcp.nrl.navy.mil

J.P. Boris
e-mail: boris@lcp.nrl.navy.mil

F.F. Grinstein
X-Computational Physics Division, Los Alamos National Laboratory, Los Alamos, NM 87545,
USA
e-mail: fgrinstein@lanl.gov

J.P. Iselin
University of Wisconsin Platteville, Platteville, WI 53818, USA

D. Hertwig
Meteorological Institute, University of Hamburg, 20146 Hamburg, Germany

unsteady buoyant flow physics are involved. The widely varying temporal and spatial scales exhaust current modeling capacities. Simulations of dispersion of airborne pollutants in urban scale scenarios must predict both the detailed airflow conditions as well as the associated behavior of the gaseous and multiphase pollutants. Reducing health risks from the accidental or deliberate release of Chemical, Biological, or Radioactive (CBR) agents and pollutants from industrial leaks, spills, and fires motivates this work. Crucial technical issues include transport model specifics, boundary condition modeling, and post-processing of the simulation results for practical use by responders to actual real-time emergencies.

Relevant physical processes to be modeled include resolving complex building vortex shedding and recirculation zones. The model must also incorporate a consistent stratified urban boundary layer with realistic wind fluctuations, solar heating including shadows from buildings and trees, aerodynamic drag, turbulence generation, and heat losses due to the presence of trees, surface heat sorption variations and turbulent heat transport. Because of the short time spans and large air volumes involved, modeling a pollutant as well mixed globally is typically not appropriate. It is important to capture the effects of unsteady, non-isothermal, buoyant flow conditions on the evolving pollutant concentration distributions. In fairly typical urban scenarios, both particulate and gaseous contaminants behave similarly insofar as transport and dispersion are concerned. Thus the contaminant spread can be simulated effectively based on appropriate pollutant tracers with suitable sources and sinks. In other cases the full details of multigroup particle distributions are required.

1.1 Established Approach: Gaussian Plume Models

Contaminant plume prediction technology currently in wide use around the world is based on Gaussian similarity solutions (“puffs”). This is a class of extended Lagrangian approximations that only really apply for large scales and flat terrain where separated-flow vortex shedding from buildings, cliffs, or mountains is absent. Diffusion is used in plume/puff models to mimic the effects of turbulent dispersion caused by the complex building geometry and wind gusts of comparable and larger size (e.g., [2–5]). These current aerosol hazard prediction tools for CBR scenarios are relatively fast running models using limited topography, weather and wind data. They give only approximate solutions that ignore the effects of flow encountering 3D structures. The air flowing over and around buildings in urban settings is fully separated. It is characterized by vortex shedding and turbulent fluctuations throughout the fluid volume. In this regime, the usual timesaving approximations such as steady-state flow, potential flow, similarity solutions, and diffusive turbulence models are largely inapplicable. Therefore, a clear need exists for high-resolution numerical models that can compute accurately the flow of contaminant gases and the deposition of contaminant droplets and particles within and around real buildings under a variety of dynamic wind and weather conditions.

1.2 Computational Fluid Dynamics Approach

Since fluid dynamic convection is the most important physical process involved in CBR transport and dispersion, the greatest care and effort should be invested in its modeling. The advantages of the Computational Fluid Dynamics (CFD) approach and representation include the ability to quantify complex geometry effects, to predict dynamic nonlinear processes faithfully, and to handle problems reliably in regimes where experiments, and therefore model validations, are impossible or impractical.

1.2.1 Standard CFD Simulations

Some “time-accurate” flow simulations that attempt to capture the urban geometry and fluid dynamic details are a direct application of standard (aerodynamic) CFD methodology to the urban-scale problem. An example is the work at Clark Atlanta University where researchers conduct finite element CFD simulations of the dispersion of a contaminant in the Atlanta, Georgia metropolitan area. The finite element model includes topology and terrain data and a typical mesh contains approximately 200 million nodes and 55 million tetrahedral elements [6]. These are grand-challenge size calculations were run on 1024 processors of a CRAY T3E. Other research groups have used similar approaches (e.g., [7, 8]). The chief difficulty with this approach for large regions is that they are computer intensive and involve severe overhead associated with mesh generation.

1.2.2 The Large-Eddy Simulation Approach

Capturing the dynamics of all relevant scales of motion, based on the numerical solution of the Navier-Stokes Equations (NSE), constitutes Direct Numerical Simulation (DNS), which is prohibitively expensive for most practical flows at moderate-to-high Reynolds Number (Re). On the other end of the CFD spectrum are the industrial standard methods such as the Reynolds-Averaged Navier-Stokes (RANS) approach, e.g., involving $k-\epsilon$ models, and other first- and second-order closure methods, which simulate only the mean flow and model the effects of all turbulent scales. These are generally unacceptable for urban CT modeling because they are unable to capture unsteady plume dynamics. Large Eddy Simulation (LES) constitutes an effective intermediate approach between DNS and the RANS methods. LES is capable of simulating flow features that cannot be handled with RANS, such as significant flow unsteadiness, and provides higher accuracy than the industrial methods at reasonable cost.

The main assumptions of LES are: (i) that transport is largely governed by large-scale unsteady convective features that can be resolved, (ii) that the less-demanding accounting of the small-scale flow features can be undertaken by using suitable sub-grid scale (SGS) models. Because the larger scale unsteady features of the flow are

expected to govern the unsteady plume dynamics in urban geometries, the LES approximation has the potential to capture many key features which the RANS methods and the various Gaussian plume methodologies cannot.

2 Monotonically Integrated LES

Traditional LES approaches seek sufficiently high-order discretization and grid resolution to ensure that effects due to numerics are sufficiently small, so that crucial LES turbulence ingredients (filtering and SGS modeling) can be resolved. In the absence of an accepted universal theory of turbulence, the development and improvement of SGS models are unavoidably pragmatic and based on the rational use of empirical information. Classical approaches [9] have included many proposals ranging from inherently-limited eddy-viscosity formulations to more sophisticated mixed models combining dissipative eddy-viscosity models with the more accurate but less stable Scale-Similarity Model. The main drawback of mixed models relates to their computational complexity and cost for the practical flows of interest at moderate-to-high Re. The shortcomings of LES methods have led many researchers to abandon the classical LES formulations and shift focus directly to the SGS modeling implicitly provided by nonlinear (monotone) convection algorithms (see, e.g., [10], for a recent survey). The idea that a suitable SGS reconstruction might be implicitly provided by discretization in a particular class of numerical schemes [11] lead to proposing the Monotonically Integrated LES (MILES) approach [12, 13]. Later theoretical studies show clearly that certain nonlinear (flux-limiting) algorithms with dissipative leading order terms have appropriate built-in (i.e. “implicit”) Sub-Grid Scale (SGS) models [14–16]. Our formal analysis and numerous tests have demonstrated that the MILES implicit tensorial SGS model is appropriate for both free shear flows and wall bounded flows. These are the conditions of most importance for CBR transport in cities.

As discussed further below, the MILES concept can be effectively used as a solid basis for CFD-based contaminant transport simulation in urban-scale scenarios, where conventional LES methods are far too expensive and RANS methods are inadequate.

3 MILES for Urban Scale Simulations

The FAST3D-CT three-dimensional flow simulation model [1, 17, 18] is based on the scalable, low dissipation Flux-Corrected Transport (FCT) convection algorithm [19, 20]. FCT is a high-order, monotone, positivity-preserving method for solving generalized continuity equations with source terms. The required monotonicity is achieved by introducing a diffusive flux and later correcting the calculated results with an antidiffusive flux modified by a flux limiter. The specific version of the convection algorithm implemented in FAST3D-CT is documented in [21].

Additional physical processes to be modeled include providing a consistent stratified urban boundary layer, realistic wind fluctuations and solar heating including shadows from buildings and trees. We must also model aerodynamic drag and heat losses due to the presence of trees, surface absorption variations and turbulent heat transport. Additional features include multi-group droplet and particle distributions with turbulent transport to surfaces as well as gravitational settling, solar chemical degradation, evaporation of airborne droplets, re lofting of particles on the ground and ground evaporation of liquids. Incorporating specific models for these processes in the simulation codes is a challenge but can be accomplished with reasonable sophistication. The primary difficulty is the effective calibration and validation of all these physical models since much of the input needed from field measurements or experiments on these processes is typically insufficient or even nonexistent. Furthermore, even though the individual models can all be validated to some extent, the larger problem of validating the overall code has to be tackled as well. Some of the principally fluid dynamics related issues are elaborated further below.

3.1 Urban Flow Modeling Issues

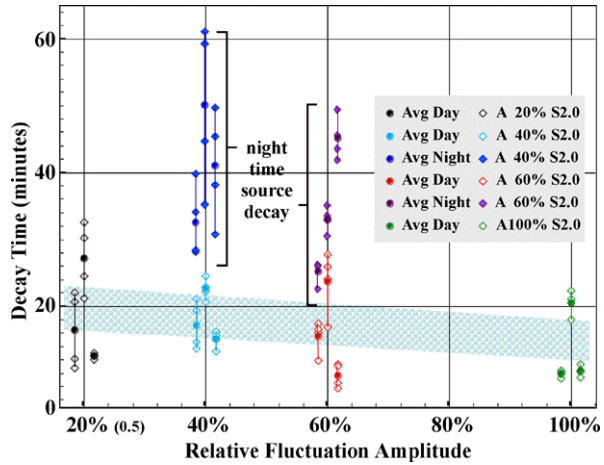
3.1.1 Atmospheric Boundary Layer Specification

We have to deal with a finite domain and so precise planetary boundary layer characterization upstream of this domain greatly affects the boundary-condition prescription required in the simulations. The weather, time-of-day, cloud cover and humidity all determine if the boundary layer is thermally stable or unstable and thus determine the level and structure of velocity fluctuations. Moreover, the fluctuating winds, present in the real world but usually not known quantitatively, are known to be important because of sensitivity studies.

In FAST3D-CT the time average of the urban boundary layer is specified analytically with parameters chosen to represent the overall thickness and inflection points characteristic of the topography and buildings upstream of the computational domain. These parameters can be determined self-consistently by computations over a wider domain, since the gross features of the urban boundary layer seem to establish themselves in a kilometer or so, but this increases the cost of simulations considerably.

A non-periodic deterministic realization of the wind fluctuations is currently being superimposed on the average velocity profiles. This realization is specified as a suitable nonlinear superposition of modes with several wavelengths and amplitudes. Significant research issues remain unresolved in this area, both observationally and computationally. Deterministic [22] and other [23] approaches to formulating turbulent inflow boundary conditions are currently being investigated in this context. The strength of the wind fluctuations, along with solar heating as described just below, are shown to be major determinants of how quickly the contaminant density flushes from the domain in time and this in turn is extremely important in emergency applications as it determines overall dosage.

Fig. 1 Effect of fluctuations on trapping of contaminants



3.1.2 Solar Heating Effects

An accurate ray-tracing algorithm that properly respects the building and tree geometry computes solar heating in FAST3D-CT. The trees and buildings cast shadows depending on the instantaneous angle to the sun. Reducing the solar constant slightly can represent atmospheric absorption above the domain of the simulation and the model will even permit emulating a time-varying cloud cover. The geometry database has a land-use variable defining the ground composition. Our simulations to date identify only two conditions, ground and water, though the model can deal with the differences between grass, dirt, concrete and blacktop given detailed enough land-use data. The simulated interaction of these various effects in actual urban scenarios has been extensively illustrated in [1].

Figure 1 shows that the rate that a contaminant is flushed out of a city by the winds can vary by a factor of four or more due to solar heating variations from day to night and due to variations in the relative strength of the wind gusts. The horizontal axis of the figure indicates the relative strength of the gusting fluctuations at the boundaries, from about 20% on the left to about 100% on the right. For each of six different “environmental” conditions, twelve ground-level sources were released, four independent realizations at each of three source locations around the urban geometry. These source locations and the scale lengths of all the wind fluctuations were held fixed for the six different runs. The value of the exponential decay time in minutes is plotted for each source and realization as a diamond-shaped symbol. The figure shows that the decay time is two or three times longer for release at night compared to the day for otherwise identical conditions. The dark blue diamonds (decay times) should be compared with the light blue and the purple diamonds compared with the red. One can also see that the decay times get systematically shorter as the wind fluctuation amplitude is increased from left to right. This is emphasized by the light blue shaded bar through the center of the four daytime data sets.

3.1.3 Tree Effects

Although we can resolve individual trees if they are large enough, their effects (i.e., aerodynamic drag, introduction of turbulent velocity fluctuations, and heat losses) are represented through modified forest canopy models [24] including effects due to the presence of foliage. For example, an effective drag-force source term for the momentum equations can be written as $F = -C_d a(z)|\mathbf{v}|\mathbf{v}$, where $C_d = 0.15$ is an isotropic drag coefficient, $a(z)$ is a seasonally-adjusted leaf area density, z is the vertical coordinate, and \mathbf{v} is the local velocity. The foliage density is represented in a fractal-like way so that fluctuations will appear even in initially laminar flows through geometrically regular stands of trees.

3.1.4 Geometry Specification

An efficient and readily accessible data stream is available to specify the building geometry data to FAST3D-CT. High-resolution (1 m or smaller) vector geometry data in the ESRI ARCVIEW data format is commercially available for most major cities. From these data, building heights are determined on a regular mesh of horizontal locations with relatively high resolution (e.g., 1 m). Similar tables for terrain, vegetation, and other land use variables can be extracted. These tables are interrogated during the mesh generation to determine which cells in the computational domain are filled with building, vegetation, or terrain. This masking process is a very efficient way to convert a simple geometric representation of an urban area to a computational grid.

This grid masking approach is used to indicate which computational cells are excluded from the calculation as well as to determine where suitable wall boundary conditions are to be applied. However, the grid masking approach is too coarse to represent rolling terrain, for which a shaved cell approach is applied. The terrain surface is represented by varying the location of the lower interface of the bottom cell. Even though this results in a terrain surface that is ultimately discontinuous, the jump between adjacent cells is very small. Operational results show that this approach works reasonably well and allow gradual changes in terrain height.

A more accurate representation of the geometry is possible with the VCE approach [25] in which all cell volume and interface areas are allowed to vary. This level of detail now begins to approach that of conventional aerodynamics CFD but it is not seen that this is necessary.

3.1.5 Wall Boundary Conditions

Appropriate wall boundary conditions must be provided so that the airflow goes around the buildings. It is not possible with the available resolution to correctly model the boundary layer on the surface. Therefore, rough-wall boundary layer models [26] are used for the surface stress, i.e., $\tau = \rho C_D (U_{||})^2$, and for the heat

transfer from the wall, $H_o = \rho C_p C_H U_{||}(\Theta - \Theta_o)$, where ρ is the mass density, C_D and C_H are coefficients characterizing the roughness and thermal properties of the walls or ground surface, $U_{||}$ is the tangential velocity at the near-wall (first grid point adjacent to the wall), C_p is the specific heat at constant pressure, and Θ and Θ_o are the potential temperature at the wall, and near-wall, respectively.

4 The MILES Implicit SGS Model

Historically, flux-limiting (flux-correcting) methods have been of particular interest in the MILES context. A flux-limiter $0 \leq \Gamma \leq 1$ combines a high-order convective flux-function \mathbf{v}_f^H that is well behaved in smooth flow regions, with a low-order dispersion-free flux-function \mathbf{v}_f^L that is well behaved near sharp gradients. Thus the total flux-function with the limiter Γ becomes $\mathbf{v}_f = \mathbf{v}_f^H - (1 - \Gamma)[\mathbf{v}_f^H - \mathbf{v}_f^L]$. Properties of the implicit SGS model in MILES are related to the choice of Γ , \mathbf{v}_f^L , and \mathbf{v}_f^H , as well as to other specific features of the algorithm [15, 16]. This is quite similar to choosing/adjusting an (explicit) SGS model in the context of conventional LES.

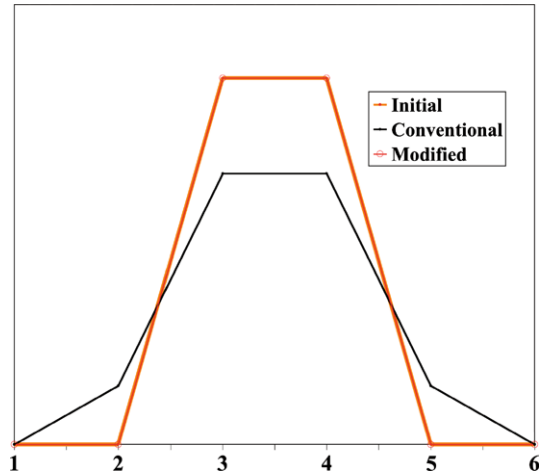
Because of its inherently less-diffusive nature, prescribing Γ based on local monotonicity constraints is a more attractive choice in developing MILES [14–16]. This is supported by our comparative channel flow studies [16] of the global performance of MILES as a function of flux limiter. For example, the van-Leer TVD limiter (e.g., [27]) was found to be too diffusive as compared to FCT [19] and GAMMA [28] limiters which produce velocity profiles that agree well with the reference DNS data.

4.1 Street Crossings

Another approach to controlling unwanted numerical diffusion is through the appropriate choice of low and high order transport algorithms. In our simulations of urban areas, the typical grid resolution is of the order of 5 to 10 meters. While this resolution is adequate to represent the larger features of the city, many of the smaller features are resolved with only one to two cells. This is true of smaller streets found in cities, which are about 10 to 20 m wide. Alleyways are even smaller. These smaller streets may be represented by only one or two cells in our computation, putting a tremendous demand on the numerical convection not to diffuse and retard the flow down these narrow streets.

By using the rough-wall boundary conditions discussed above instead of no-slip boundary conditions, the flow can proceed unhampered down a single street even for streets that are only one cell wide. However, if there is another street intersecting the first, it was found that the flow essentially stagnates at this intersection. The problem only occurs when dealing with streets which are 1–2 cells wide and not with wider

Fig. 2 Advected quantity as function of grid index for both the conventional and modified low-order schemes



streets. After careful inspection, it was determined that the problem arose due to the form of the diffusion term in the low-order solution in the standard FCT algorithm, LCPFCT [21], used in the FAST3D-CT code.

The traditional low-order component of FCT introduces numerical diffusion even when the velocity goes to zero (as in the cross street) [21]. In normal situations, the flux limiter is able to locate an adjacent cell that has not been disturbed by the diffusion in the low-order method and is able to restore the solution to its original undiffused value. However, when the streets are 1–2 cells wide, the region of high velocity is diffused by low-order transport and there are no cells remaining at the higher velocity (Fig. 2). Thus the flux limiter cannot restore the solution in these cells to the original high value.

A solution to this problem lay in changing the form of the diffusion in the low-order method. In LCPFCT, the algorithmic diffusion coefficient for the low-order scheme is given by $\nu = \frac{1}{6} + \frac{1}{3}\varepsilon^2$, where the Courant number $\varepsilon = |U|\Delta t/\Delta x$. Note that ν does not go to zero even when U goes to zero (as in the cross street). The simplest less-diffusive low-order algorithm which ensures monotonicity is the upwind method previously used in the formal MILES analysis (e.g., [16]) for which the diffusion coefficient is given by $\nu_{upwind} = \frac{1}{2}|\varepsilon|$, which has the desired form for ν . When the diffusion coefficient in the low-order component of FCT is replaced by ν_{upwind} , the flow no longer stagnates at the intersection of streets (Fig. 2). This variation of the low-order method is only used for the momentum equations. It is not required for the density equation, since the density is almost constant everywhere. With this modification of the low-order method, the global properties of the transport algorithm were altered sufficiently to address this problem peculiar of under-resolved flows in urban areas.

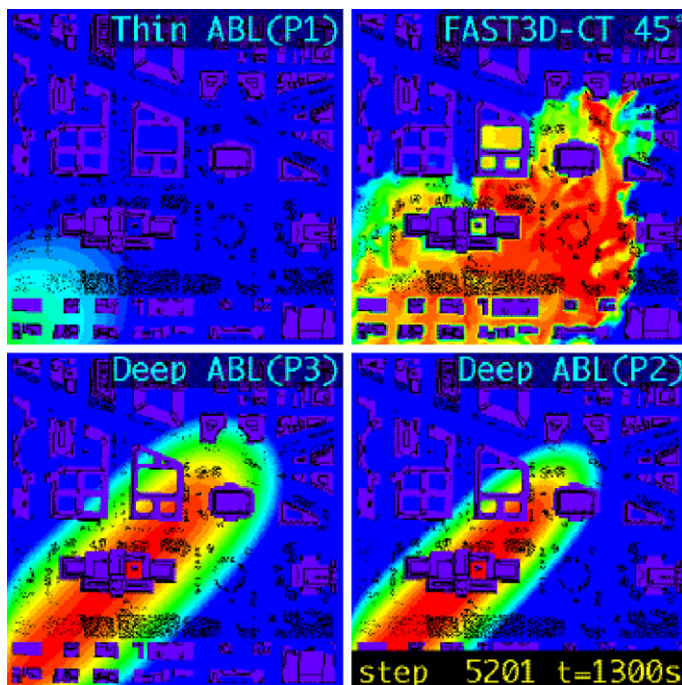


Fig. 3 Comparison of Gaussian Plume and FAST3D-CT simulations

5 Practical Examples

5.1 Gaussian Lagrangian vs. Unsteady 3D Solutions

Gaussian atmospheric transport and dispersion schemes are characterized by some initial direct spreading of the contaminant upwind by the diffusion, regardless of wind speed. The characteristic differences between the three Gaussian similarity solutions in Fig. 3 are similar to the differences between different Gaussian plume/puff models. None of these approximate, idealized solutions has the correct shape, trapping behavior, or plume width when compared to the FAST3D-CT simulation shown in the upper-right panel of the Fig. 3. The contaminant gets trapped in the recirculation zones behind buildings and continues to spread laterally long after simpler models say the cloud has moved on.

More detailed comparisons using actual “common use” puff/plume models (e.g., [29]) show a range of results depending on how much of the 3D urban boundary layer information from the detailed simulation is incorporated in the Gaussian model. Though building-generated aerodynamic asymmetries cannot be replicated, crosswind spreading and downwind drift can be approximately matched given enough free parameters. However, because the detailed simulations show that the plume expands like an angular sector away from the source, Gaussian models show

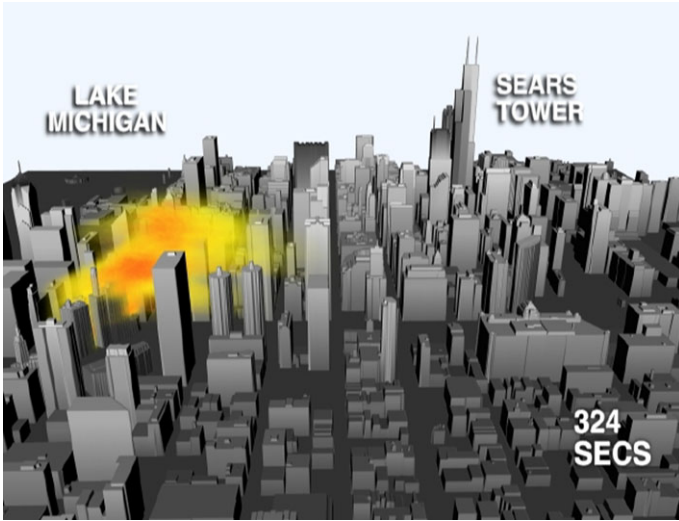


Fig. 4 View of contaminant release looking east toward downtown Chicago

too rapid a lateral spreading in the vicinity of the source to provide a plume that is approximately the correct width downwind.

5.2 *Unsteady 3D Solution—Chicago*

The city of Chicago is typical of a large, densely populated metropolitan area in the United States. The streets in the downtown area are laid out in a grid-like fashion, and are relatively narrow. The buildings are very tall but with small footprints. For example, the Sears tower is now the tallest building in the U.S.

Figures 4–6 show different views of a contaminant cloud from a FAST3D-CT simulation of downtown Chicago using a $360 \times 360 \times 55$ grid (6 m resolution). A 3 m/s wind off the lake from the east blows contaminant across a portion of the detailed urban geometry data set required for accurate flow simulations. One feature that is very apparent from these figures is that the contaminant is lofted rapidly above the tops of the majority of the buildings. This vertical spreading of the contaminant is solely due to the geometrical effect of the buildings. This behavior has also been observed in other simulations in which the buildings are not as tall.

Placement of the contaminant source can have a very nonlinear effect on the dispersion characteristics. Figures 7 and 8 show results of identical simulations with the exception of the contaminant release locations, which are shown by the red markers. The blue markers show the release location in the other simulation. Although the release locations differed by less than 0.5 km the dispersion characteristics are markedly different. The narrower dispersion pattern in Fig. 7 is likely caused by

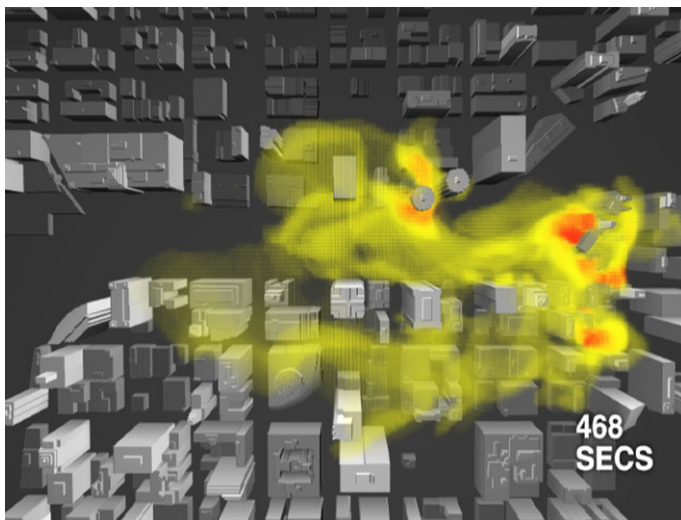


Fig. 5 Overhead view of contaminant concentrations over Chicago River

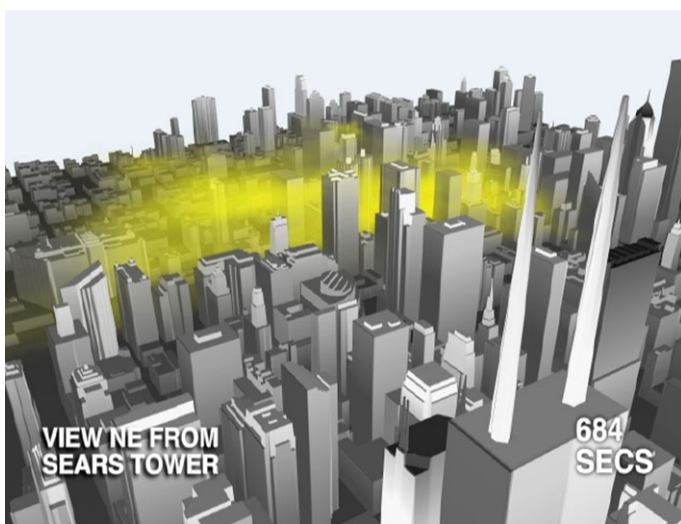


Fig. 6 View of contaminant from the Sears tower

a channeling effect of the Chicago River where velocities are higher. The wider dispersion pattern in Fig. 8 is likely due to a combination of flow deflection and recirculation of the flow from the building geometry. This behavior may also be dependent on release time. Work is continuing to determine the function dependence on location and release time. However, it is clear that spatially averaged parameteri-

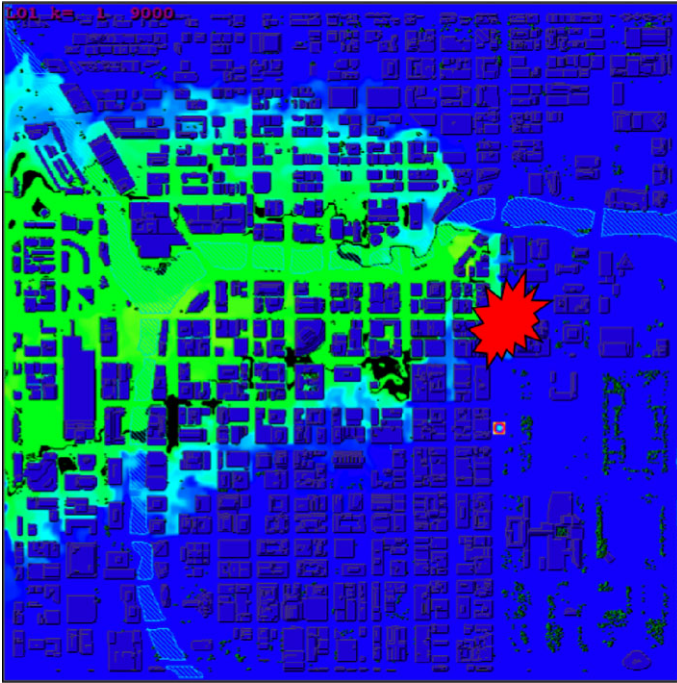


Fig. 7 Contaminant dispersion at ground level for release close to Chicago River

zations of urban surface characteristics will be unable to account for these nonlinear effects.

Additional simulations for Chicago were used to examine the effect of the modified low-order component of FCT as described in Sect. 4.1. Figure 9 shows the contaminant at ground level 9 minutes after release using the standard FCT algorithm LCPFCT [21]. The channeling effect of the Chicago River is quite dominant, though some lateral spreading occurs as well. The calculations were then repeated with the modified low-order method. These results are shown in Fig. 10. It is immediately apparent that the lateral spreading is much larger in this second case and that the cloud also propagates more rapidly downstream. These effects can be attributed to the lowered numerical diffusion in the cross-stream direction and the consequent lowering of numerical diffusion overall. Figure 11 shows the velocity (averaged horizontally over the computational domain) and RMS fluctuation profiles for both LCPFCT and the modified low-order scheme. The modified method has higher values for both velocity and RMS fluctuation. This is consistent with the observation of increased downstream and cross-stream propagation of the contaminant.

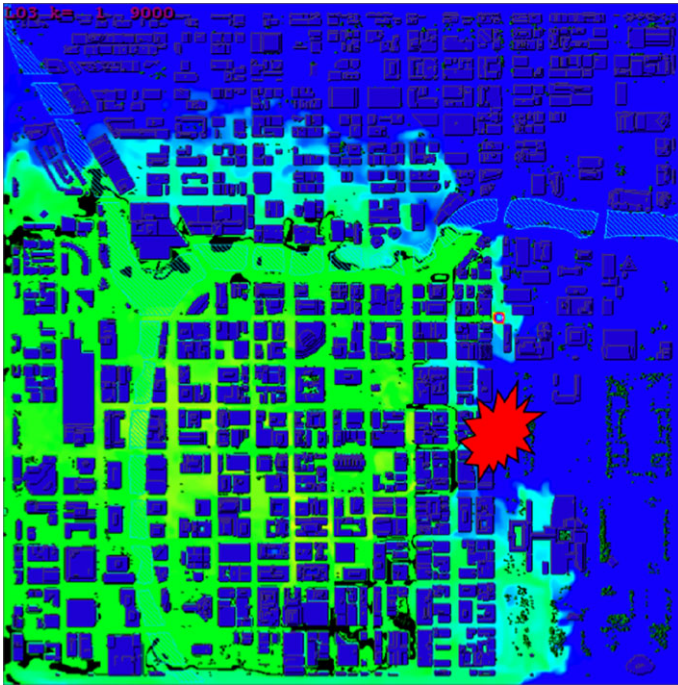


Fig. 8 Contaminant dispersion at ground level for release further from Chicago River

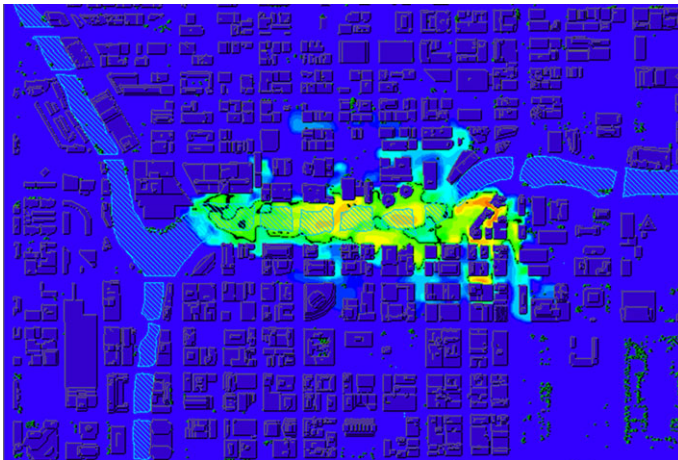


Fig. 9 Contaminant dispersion using standard low-order method

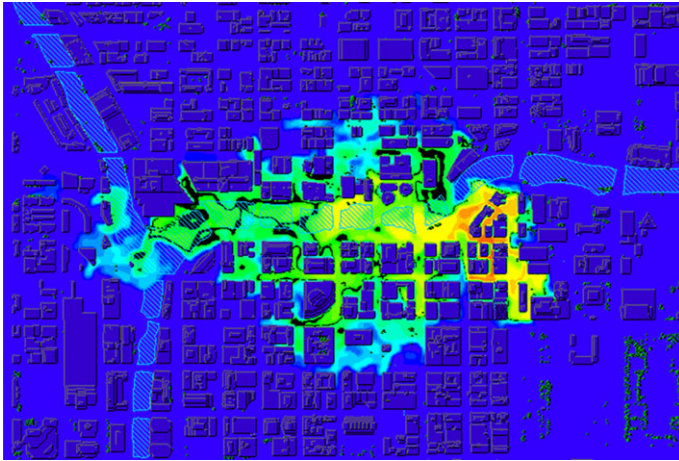
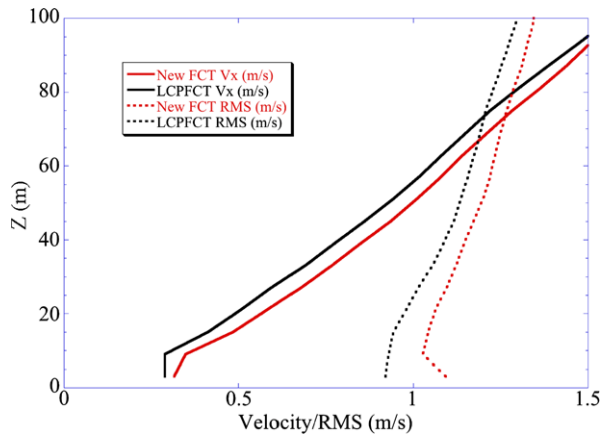


Fig. 10 Contaminant dispersion using modified low-order method

Fig. 11 Comparison of the standard and modified low-order method: velocity and RMS fluctuation profiles



5.3 Unsteady 3D Solution—Baghdad

Baghdad is rather typical of capital cities—it has large, spread-out governmental buildings, parks and monuments. There is no large dense urban core with tall buildings but there are several greater than 20 story buildings that are spread out. Residential areas are mostly suburban with some high-rise housing. This city structure is quite different from Chicago with its skyscrapers. A limited amount of high-resolution building data was available from a government-related source; however this data only included the largest buildings and covered a fraction of the area of the city. Large portions, especially residential areas, were not covered. Also, land-use data (trees, water, etc.) were not available in high-resolution form.

The missing data was constructed manually, primarily from commercially available satellite photographs of the city. These photographs had sufficient resolution

to discern trees, water, and even types of housing. “Synthetic” buildings were generated to represent areas not covered by the available high-resolution data. Typical building heights and shapes found in suburbs were assigned at random to suburban regions. One of the difficulties not typically found in CFD calculations which proved to be a challenge was to ensure proper geo-referencing of the data, i.e., ensure everything lined up. This is especially severe when working from photographs that do not have a uniform resolution, and may sometimes not have the proper desired orientation.

5.3.1 In-Situ Validation

One of the obvious difficulties that arise for simulations of urban areas is that of validation of results. Experimental data is rarely available, and what little that is available is extremely limited in scope and coverage. The type and extent of data that is available restrict the quality of the validation effort. For Baghdad, no specific field measurements are available. However, just prior to the start of the war in Iraq, large trenches filled with oil were set ablaze in hope that the smoke would obscure targets. The smoke from one such fire provided an opportunity to at least visually “validate” our plume calculations. Figure 12 is a satellite photograph (courtesy DigitalGlobe) of the smoke from a trench fire near the monument to the Unknown Soldier. Figures 13 and 14 show the results from our simulations of the event. Color contours of the tracer gas are shown. The weather conditions for that day were given as “light wind from northwest.” The simulations were carried with nominal wind speed of 3 m/s at 340°. An important unknown that had to be estimated is the level of fluctuation in the wind. The simulation depicted in Fig. 13 used a low level of fluctuation, which is consistent with the light steady winds typically found in March in the area. In order to investigate the importance of wind fluctuations, a higher level of fluctuations was simulated as shown in Fig. 14, which had fluctuations four times as high in amplitude as the baseline case (Fig. 13). As expected, the plume does spread slightly further. However, for low wind fluctuations, the spreading is largely controlled by the geometry of the city—an effect that becomes more dominant in dense urban areas. These calculations show that while a good knowledge of the weather is required for accurate predictions, in order to predict a worst-case scenario it is possible to select the appropriate parameters without perfect knowledge of all input conditions.

5.4 Detailed Validation Study—Hamburg, Germany

In a systematic study FAST3D-CT results of turbulent flow in the inner city of Hamburg, Germany, are being compared to reference measurements from a boundary-layer wind tunnel experiment. The urban structure is characteristic for northern and central European cities with complex crossings and courtyards. The focus of the validation exercise is the comparison of time-series information and the characterization of turbulent flow structures within and above the urban canopy.



Fig. 12 Smoke plume from oil fire in Baghdad

5.4.1 Experimental and Numerical Methods

Laboratory measurements in specialized boundary-layer wind tunnels can provide an ideal validation data basis supplementary to information from field sites. Well definable and controllable boundary conditions together with the potential to repeat experimental runs under the same constraints result in high statistical confidence levels of the measured quantities. The reference measurements were performed in the boundary-layer wind tunnel facility at the University of Hamburg. The wind-tunnel model comprises the city center of Hamburg together with industrial harbor sites that are separated from the downtown area by the river Elbe. In total, the model domain encompasses an area of $3.7 \text{ km} \times 1.4 \text{ km}$ in full-scale dimension. The physical model was built on a scale of 1:350, including terrain and a 3.5 m high water front. Effects of urban greenery are not accounted for. Figure 15 shows a photograph

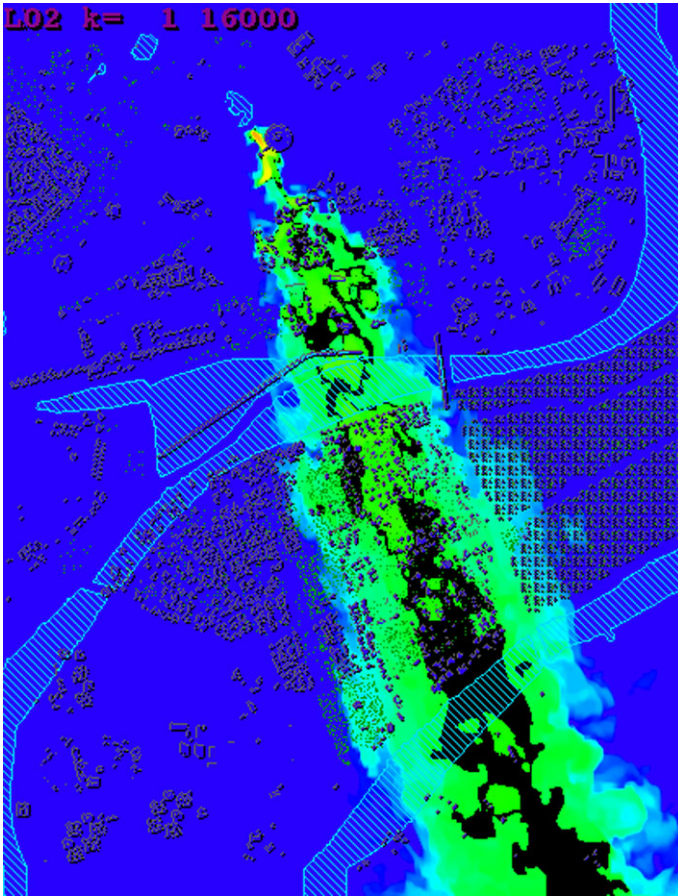


Fig. 13 Simulation of smoke plume. Low wind fluctuations

of the wind-tunnel model. The flow is approaching from the southwest (235°), mirroring a quite frequent meteorological condition for that area. The inflow boundary layer profiles were physically modeled to feature urban (i.e. very rough) turbulence characteristics (wind profile exponent $\alpha \approx 0.29$; roughness length $z_0 \approx 1.5$ m) under neutral atmospheric stratification. All flow measurements were conducted using non-intrusive 2D laser Doppler velocimetry.

The 3D FAST3D-CT simulation for Hamburg was performed on a $4 \text{ km} \times 4 \text{ km}$ region of the inner city with 2.5 m grid resolution. The calculation was run on 64 CPUs of a SGI Altix computer and took more than three weeks to generate over 4 hours of real time data. The average wind direction is 235° rotated clockwise from due south. The wind speed was approximately 7 m/s at a height of 190 m. To match the FAST3D-CT conditions with the wind-tunnel experiments as closely as possible, all temperature related effects such as buoyancy and surface heating as

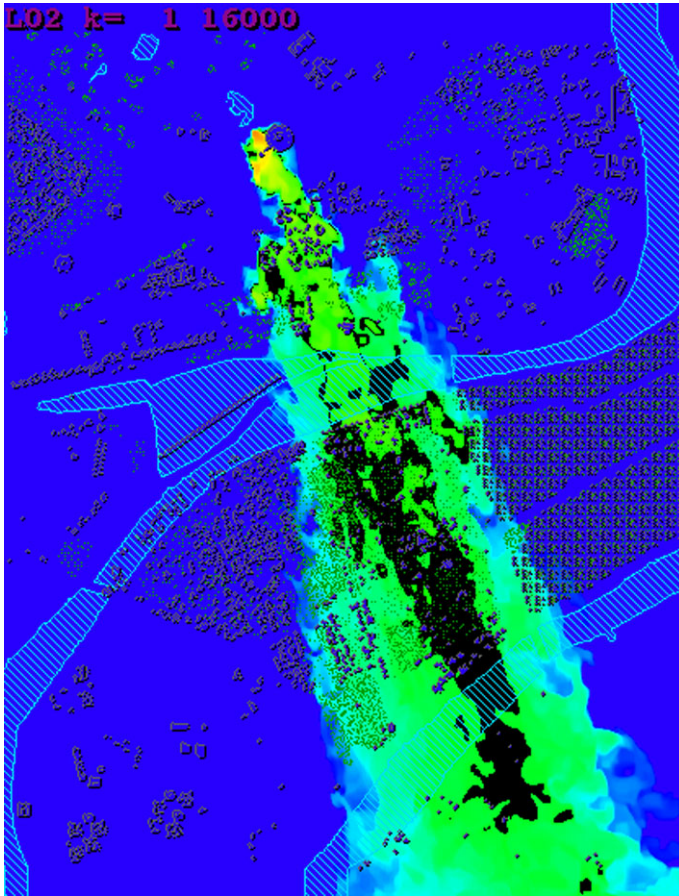


Fig. 14 Simulation of smoke plume. High wind fluctuations

well as drag effects of trees have been turned off. Time-dependent wind data were collected every 0.5 seconds at various heights up to 130 m.

For the validation exercise, 22 measurement locations within the model domain were chosen, including narrow street canyons, complex intersections, and measurement points close to the ground. This selection was made to represent areas of the city that are characteristic of urban flow situations and also pose challenges to numerical models. Velocity measurements were made in the numerical calculations to match the specified locations in the wind-tunnel experiment as closely as possible. The nearest neighbor extraction was chosen in order to avoid contamination of the results by interpolating data in order to have an exact spatial match. This procedure in some cases led to slight offsets of the x , y , and z positions of the comparison points that were in the range of a few centimeters up to a maximum of 1.75 m. Experimental and numerical data were normalized by referencing all velocities and their derivatives to a reference wind speed at a fixed location. This monitoring point

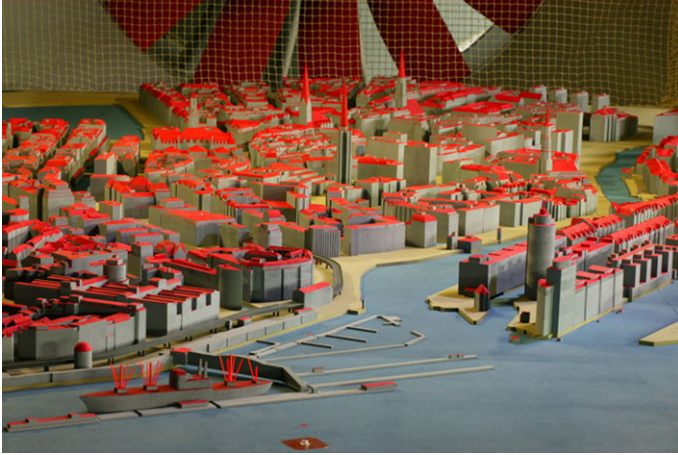


Fig. 15 Urban model of the inner city of Hamburg mounted in the boundary-layer wind-tunnel. View is from the inflow direction of 235° . Courtesy of the Environmental Wind Tunnel Laboratory at the University of Hamburg

was defined at a height of 49 m above the river Elbe at approximately 1 km upstream from the city center.

5.5 Mean Flow Comparison

The validation started from a comparison of mean flow characteristics in terms of time-averaged velocities. Figure 16 shows comparisons of vertical profiles of the streamwise velocity component from wind-tunnel measurements and FAST3D-CT simulations. In these and the following figures measurement locations are indicated by red dots on the city maps. The profile positions differ in the arrangement of the surrounding buildings. Figure 16(a) shows velocity profiles above the river Elbe (the (x, y) -location is identical with the reference point). Being situated well upstream of the densely built-up city center, the good agreement between experimental and numerical profiles mirrors a good match of the mean inflow conditions. A good agreement is also found for positions at which the flow is strongly influenced by the building structure. Figure 16(b) shows a profile measured in a very narrow street canyon. In Fig. 16(c), the measurement position is located in an open plaza exhibiting a strong recirculation regime that is captured quite well by the code. Measurements shown in Figs. 16(d)–(f) were conducted at intersections that trigger complex flow behavior. At elevations below the mean building height (approx. $H_{\text{mean}} \approx 35$ m by averaging over the city center) there is a slight trend towards an underprediction of velocities, whereas higher wind speeds than in the reference are observed at heights larger than $2.5 H_{\text{mean}}$. The close proximity of building walls and the wall model used in the simulation might explain the slight offsets found within the street

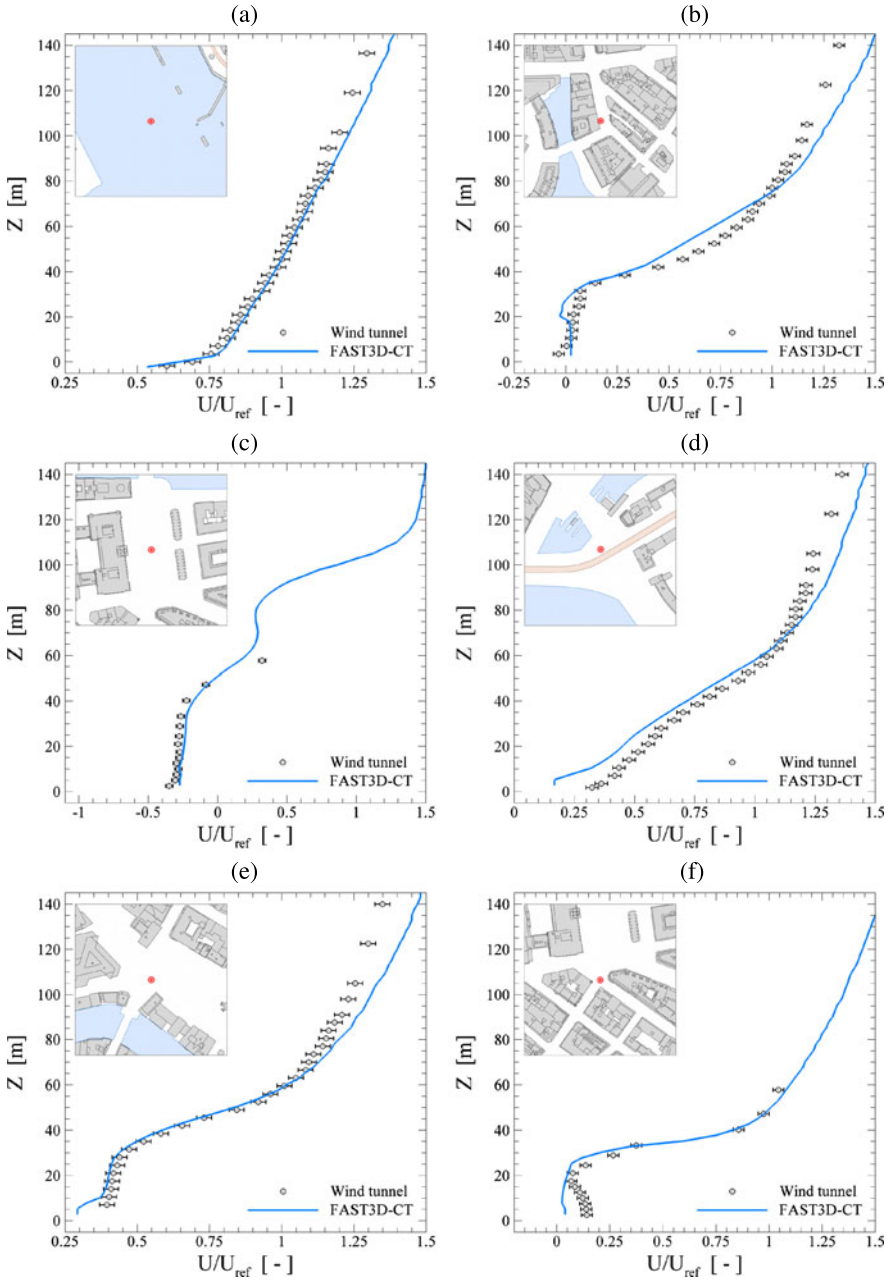


Fig. 16 Comparison of mean streamwise velocity profiles from wind-tunnel measurements (*circles*) and numerical simulations with FAST3D-CT (*lines*) at different locations within the city (a)–(f). Scatter bars attached to the experimental values represent the reproducibility of the data based on repetition measurements. The incoming flow is from left to right

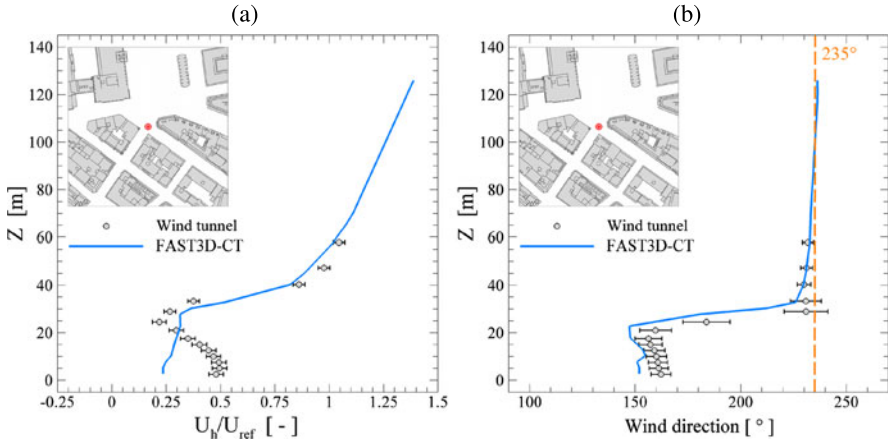


Fig. 17 Mean horizontal wind speed (a) and wind direction profiles (b) from wind-tunnel measurements (circles) and FAST3D-CT calculations (lines)

canyon. The stronger acceleration well above the canopy might reflect an excess of TKE in the numerical inflow prescription or the specific implementation of the upper numerical boundary.

5.6 Time Series Analysis

Next, experimental and numerical time series were analyzed in terms of frequency distributions and turbulent energy spectra. It has to be noted that both signals differ in their length and their time resolution under full-scale conditions. While the 170 s measurement time in the wind tunnel results in a full-scale duration of 16.5 h, the duration of the numerical time series is 4.5 h. Especially at low elevations within street canyons the full-scale temporal resolution of 2 Hz of the FAST3D-CT signals is better than the scaled wind-tunnel data rate that is strongly affected by the local flow seeding conditions.

First, the frequency distributions of instantaneous horizontal wind speeds and wind directions were evaluated. The mean horizontal wind speeds U_h and wind directions are compared in terms of vertical profiles shown in Figs. 17(a) and 17(b), respectively. At each of the profile heights, the fluctuations about these means were investigated. Figure 18 shows wind-rose diagrams of horizontal wind speeds and directions that were observed (Fig. 18(a)) and simulated (Fig. 18(b)) at four different heights within and above the street canyon. The wind-rose bars display the fractional frequency at which certain wind speeds (color-coded) were observed from the respective class of wind directions. At first view, the graphs show that the model predicts the deflection of wind directions inside the canopy quite well, together with the adjustment to the wind direction of the inflow at rooftop level and well above at 57.75 m (i.e. $1.65 H_{\text{mean}}$). The spread about the central direction is largest at rooftop

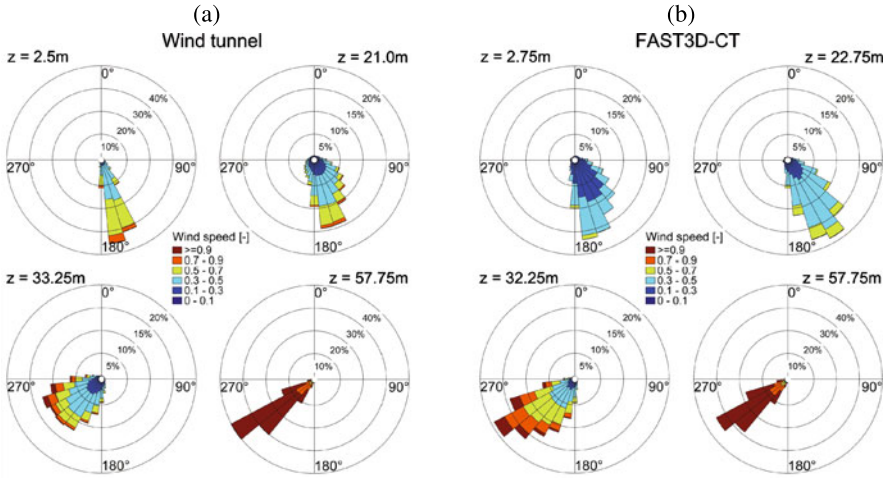


Fig. 18 Wind-rose diagrams showing frequency distributions of horizontal wind speeds and wind directions for wind-tunnel measurements (a) and FAST3D-CT simulations (b) at four different heights within and above a street canyon

height and smallest at the highest elevation in both the experiment and the simulation. However, discrepancies in velocity magnitudes are observed inside the canopy, especially for the lowermost point at 2.5 m (experimental) and 2.75 m (simulation), respectively. As discussed earlier in connection with the mean flow validation, the lower magnitudes are most likely due to the influence of wall boundary conditions prescribed at the ground and at upright building surfaces. Despite these differences the analysis indicates that the LES code is able to reproduce the directional fluctuation levels caused by unsteady flow effects quite reliably.

Auto-spectral energy densities of the turbulent streamwise velocity component are studied in order to analyze the spectral content associated with different eddy structures in the flow. The spectra were obtained using an FFT algorithm. Figure 19 shows scaled frequency spectra obtained from numerical and experimental velocities at various locations at heights of 17.5 m ($\approx 0.5 H_{\text{mean}}$) in Figs. 19(a) and 19(b) and 45.5 m ($\approx 1.3 H_{\text{mean}}$) in Figs. 19(c) and 19(d). A very good agreement of the production and energy-containing range of the spectra is found at all positions. The energetic peaks associated with integral length scale eddies coincide very well for the measurements shown in Figs. 19(b) and 19(d), whereas at the other positions the peaks are shifted for more than a decade towards higher frequencies. In order to investigate this, further analyses might concentrate on comparisons of integral length scales that can be determined from autocorrelation time scales invoking Taylor’s hypothesis.

Common to all of the numerical spectra is their fast roll-off in the high frequency range that marks the onset of the influence of the nonlinear flux-limiting (MILES) and numerical dissipation. At most of the investigated locations this influence becomes noticeable approximately one decade after the spectral peak was reached

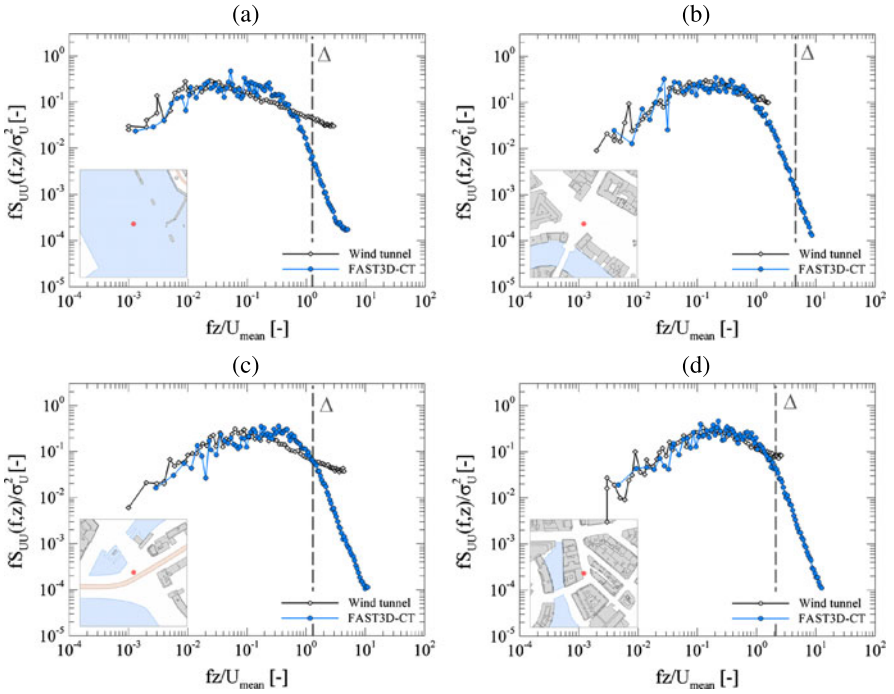


Fig. 19 Auto-spectral energy densities of the fluctuating streamwise velocity component from wind-tunnel measurements and simulations with FAST3D-CT at various locations within the city at heights of (a)–(b) 17.5 m ($\approx 0.5 H_{\text{mean}}$) and (c)–(d) 45.5 m ($\approx 1.3 H_{\text{mean}}$). The dashed lines separate the low frequency parts of the spectra that can be directly resolved by the numerical model given the grid resolution of $\Delta = 2.5$ m and the respective mean wind speeds from the subgrid-scales affected by numerical diffusion

resulting in a shortened extent of the inertial range. These urban flows are characterized by local production of turbulence at scales very close to the grid cutoff.

In consideration of the fact that FAST3D-CT was particularly designed to simulate dispersion processes in urban areas, the very good match of the energy-containing ranges associated with eddies that play a dominant role for scalar transport confirms the model's fitness for that purpose. However, it should be studied whether an extension of the inertial range is possible in order to add to the physical fidelity of the LES, even though this is not expected to contribute appreciably to the dispersion of contaminants.

6 Concluding Remarks

Physically realistic urban simulations are now possible but still require some compromises due to time, computer, and manpower resource limitations. The necessary

trade-offs result in sometimes using simpler models, numerical algorithms, or geometry representations than we would wish. We know that the quality of the spatially and time-varying boundary conditions imposed, that is, the fluctuating winds, require improvement. However, detailed time-dependent wind field observations at key locations can be processed suitably to provide initial and boundary conditions and, at the least, can be used for global validation (e.g., [23]).

We believe that the building and large-scale fluid dynamics effects that can be presently captured govern the turbulent dispersion, and expect that the computed predictions will get better in time because the MILES methodology is convergent. However, there is considerable room to improve both the numerical implementation and the understanding of the backscatter that is included implicitly by through the MILES methodology.

Inherent uncertainties in simulation inputs and model parameters beyond the environmental variability also lead to errors that need to be further quantified by comparison with high quality reference data. Judicious choice of test problems for calibration of models and numerical algorithms are essential and sensitivity analyses help to determine the most important processes requiring improvement. In spite of inherent uncertainties and model trade-offs it is possible to achieve a significant degree predictability. For example, today, the biggest errors in comparing to field trials are associated with determining the actual wind profile and direction during the trial.

The FAST3D-CT simulation model can be used to simulate sensor and system response to postulated threats, to evaluate and optimize new systems, and to conduct sensitivity studies for relevant processes and parameters. Moreover, the simulations can constitute a virtual test range for micro- and nano-scale atmospheric fluid dynamics and aerosol physics, to interpret and support field experiments, and to evaluate, calibrate, and support simpler models.

Figure 5 illustrates the critical dilemma in the CT context: unsteady 3D urban-scenario flow simulations are currently feasible—but they are still expensive and require a degree of expertise to perform. First responders and emergency managers on site for contaminant release threats cannot afford to wait while actual simulations and data post-processing are being carried out. A concept addressing this problem [1, 30] carries out 3D unsteady simulations in advance and pre-computes compressed databases for specific urban areas based on suitable (e.g., historical, seasonally adjusted) assumed weather, wind conditions, and distributed test-sources. The relevant information is summarized as *Dispersion nomograph*TM data so that it can be readily used through portable devices, in conjunction with urban sensors providing current observational information regarding local contaminant concentrations, wind speed, direction, and relative strength of wind fluctuations.

Acknowledgements The authors wish to thank Bob Doyle and the many members of NRL's LCP&FD for helpful technical discussions and scientific contributions to this effort. Further thanks are expressed to the members of the Environmental Wind Tunnel Laboratory at the University of Hamburg that contributed to the work within the Hamburg Pilot Project. Aspects of the work presented here were supported by ONR through NRL, the DoD High Performance Computing Modernization Office, DARPA, MDA and the German Federal Office of Civil Protection and Disaster Assistance (BBK) as well as the City of Hamburg, Germany.

References

1. Boris, J.P.: The threat of chemical and biological terrorism: preparing a response. *Comput. Sci. Eng.*, **4**, 22–32 (2002)
2. Hazard prediction and assessment capability. http://www.dtra.mil/td/acecenter/td_hpac_fact.html
3. Bauer, T., Wolski, M.: Software User's Manual for the Chemical/Biological Agent Vapor, Liquid, and Solid Tracking (VLSTRACK) Computer Model, Version 3.1. NSWCCD/TR-01/83 (April 2001)
4. ALOHA Users Manual: (1999). Available for download at: <http://www.epa.gov/ceppo/cameo/pubs/aloha.pdf>. Additional information: <http://response.restoration.noaa.gov/cameo/aloha.html>
5. Leone, J.M., Nasstrom, J.S., Maddix, D.M., Larsen, D.J., Sugiyama, G.: LODI User's Guide, Version 1.0. Lawrence Livermore National Laboratory, Livermore (2001)
6. Aliabadi, S., Watts, M.: Contaminant propagation in battlespace environments and urban areas. *AHPCRC Bull.* **12**(4) (2002). <http://www.ahpcrc.org/publications/archives/v12n4/Story3/>
7. Chan, S.: FEM3C—an Improved Three-Dimensional Heavy-Gas Dispersion Model: User's Manual. UCRL-MA-116567, Lawrence Livermore National Laboratory, Livermore (1994) Rev. 1
8. Camelli, F., Löhner, R.: Assessing maximum possible damage for release events. In: Seventh Annual George Mason University Transport and Dispersion Modeling Workshop, June 2003
9. Sagaut, P.: *Large Eddy Simulation for Incompressible Flows*, 3rd edn. Springer, New York (2006)
10. Grinstein, F.F., Margolin, L.G., Rider, W.J. (eds.): *Implicit Large Eddy Simulation: Computing Turbulent Flow Dynamics*, 2nd Printing. Cambridge University Press, New York (2010)
11. Boris, J.P.: On large eddy simulation using subgrid turbulence models. In: Lumley, J.L. (ed.) *Whither Turbulence? Turbulence at the Crossroads*, p. 344. Springer, New York (1989)
12. Boris, J.P., Grinstein, F.F., Oran, E.S., Kolbe, R.J.: New insights into large eddy simulation. *Fluid Dyn. Res.* **10**, 199–228 (1992)
13. Oran, E.S., Boris, J.P.: Computing turbulent shear flows—a convenient conspiracy. *Comput. Phys.* **7**(5), 523–533 (1993)
14. Fureby, C., Grinstein, F.F.: Monotonically integrated large eddy simulation of free shear flows. *AIAA J.* **37**, 544–556 (1999)
15. Fureby, C., Grinstein, F.F.: Large eddy simulation of high Reynolds-number free & wall-bounded flows. *J. Comput. Phys.* **181**, 68–97 (2002)
16. Grinstein, F.F., Fureby, C.: Recent progress on MILES for high Reynolds-number flows. *J. Fluids Eng.* **124**, 848–861 (2002)
17. Cybyk, B.Z., Boris, J.P., Young, T.R., Lind, C.A., Landsberg, A.M.: A detailed contaminant transport model for facility hazard assessment in urban areas. AIAA Paper 99-3441 (1999)
18. Cybyk, B.Z., Boris, J.P., Young, T.R., Emery, M.H., Cheatham, S.A.: Simulation of fluid dynamics around complex urban geometries. AIAA Paper 2001-0803 (2001)
19. Boris, J.P., Book, D.L.: Flux-corrected transport I, SHASTA, a fluid transport algorithm that works. *J. Comput. Phys.* **11**, 8–69 (1973)
20. Boris, J.P., Book, D.L.: Solution of the continuity equation by the method of flux-corrected transport. *Methods Comput. Phys.* **16**, 85–129 (1976)
21. Boris, J.P., Landsberg, A.M., Oran, E.S., Gardner, J.H.: LCPFCT—a flux-corrected transport algorithm for solving generalized continuity equations. U.S. Naval Research Laboratory Memorandum Report NRL/MR/6410-93-7192 (1993)
22. Mayor, S.D., Spalart, P.R., Tripoli, G.J.: Application of a perturbation recycling method in the large-eddy simulation of a mesoscale convective internal boundary layer. *J. Atmos. Sci.* **59**, 2385–2395 (2002)
23. Bonnet, J.P., Coiffet, C., Delville, J., Druault, Ph., Lamballais, E., Largeau, J.F., Lardeau, S., Perret, L.: The generation of realistic 3D unsteady inlet conditions for LES. AIAA 2003-0065 (2002)

24. Dwyer, M.J., Patton, E.G., Shaw, R.H.: Turbulent kinetic energy budgets from a large-eddy simulation of flow above and within a forest canopy. *Bound.-Layer Meteorol.* **84**, 23–43 (1997)
25. Landsberg, A.M., Young, T.R., Boris, J.P.: An efficient parallel method for solving flows in complex three-dimensional geometries. AIAA Paper 94-0413 (1994)
26. Pal Arya, S.: *Introduction to Micrometeorology*. Academic Press, San Diego (1998)
27. Hirsch, C.: *Numerical Computation of Internal and External Flows*. Wiley, New York (1999)
28. Jasak, H., Weller, H.G., Gosman, A.D.: High resolution NVD differencing scheme for arbitrarily unstructured meshes. *Int. J. Numer. Methods Fluids* **31**, 431–449 (1999)
29. Pullen, J., Boris, J.P., Young, T.R., Patnaik, G., Iselin, J.P.: Comparing studies of plume morphology using a puff model and an urban high-resolution model. In: *Seventh Annual George Mason University Transport and Dispersion Modeling Workshop*, June 2003
30. Boris, J.P., Obenschain, K., Patnaik, G., Young, T.R.: CT-ANALYSTTM, fast and accurate CBR emergency assessment. In: *Proceedings of the 2nd International Conference on Battle Management*, Williamsburg, VA, November 4–8, 2002